Critical and compensation temperatures for the mixed spin-3/2 and spin-5/2 Ising model

N. De La Espriella Vélez and C. Ortega López,
Grupo Avanzado de Materiales y Sistemas Complejos - GAMASCO,
Departamento de Física, Universidad de Córdoba, Montería, Colombia.
e-mail: ndelae52@gmail.com

F. Torres Hoyos
Departamento de Física, Universidad de Córdoba, Montería, Colombia

Recibido el 24 de agosto de 2012; aceptado el 5 de noviembre de 2012

We have studied the critical and compensation temperatures of a ferrimagnetic Ising system with mixed spins S_i^A= $\pm 3/2, \pm 1/2$ and σ_j^B = $\pm 5/2, \pm 3/2, \pm 1/2$, by using Monte Carlo simulations. The spins are alternated on a square lattice, such that nearest neighbor interactions occur between different spins ($S_i^A \leftrightarrow \sigma_j^B$) and next nearest neighbors interactions between spins of the same type ($S_i^A \leftrightarrow S_j^A$). We investigate the effects of crystal field D and the J_2 ferromagnetic coupling of spins S_i^A on the critical and compensation temperatures of the system, calculating the phase diagrams at finite temperature at the ($D/|J_1|, k_BT/|J_1|$) and ($J_2/|J_1|, k_BT/|J_1|$) planes. When the Hamiltonian includes antiferromagnetic couplings between spins S_i^A and σ_j^B, ferromagnetic between spins S_i^A and the term of single ion anisotropy D, the system presents compensation temperatures in a certain range of parameters, which depend on the intensity of the ferromagnetic interaction of spins S_i^A.

Keywords: Ising system; Monte Carlo; critical temperatures; compensation temperatures; crystal field.

PACS: 68.65.Cd; 77.84.Bw; 71.15.Mb; 71.15.Ap

1. Introduction

Simulation and numerical study by mixed Ising spin models in various molecular magnets, in equilibrium and nonequilibrium [1–4], has become an important theoretical tool for analysis and comprehension [5–8]. Currently these models are proposed as an excellent laboratory for understanding of certain thermomagnetic properties of some magnetic molecular materials two and three dimensional [9, 10], among the highlighting ferrimagnetic ordering [11–14], presence of giant magnetic moments of some doped materials [15], high critical temperatures, photoinduced magnetization [11, 16], magnetic ordering at room temperature, spontaneous magnetic moments, magnetoelastic transitions [4, 8], tricritical phenomena [17, 18], character changes of the phase transition from a second order to first order [19], reentrant and double reentrant phenomena [20–22], and the appearance of compensation temperatures in a certain range of concentration of the components [23]: temperatures below the critical temperature where the magnetizations of the sublattices have equal magnitude and opposite sign so that the total magnetization is zero. Experimentally, were obtained some compensation temperature measurements in Fe_3O_4 and Mn_3O_4 superlattices [24], and studies by Kageyama *et al.* [25] on the magnetic properties of nickel (II) formate dihydrate compound N_i(H-COO)$_2\cdot 2H_2O$, show that in addition to the phenomenon of magnetization reversal, presents compensation points. In like manner, previous studies show that at the compensation temperature, the coercivity of a material increases dramatically and at this point only is required a small conductor field to invert the sign of the magnetization [26–30]. This episode has interesting technological applications, especially in the magneto-optical recording [31, 32]. Other systems of interesting magnetic behavior, which have been studied using mixed Ising spin models are magnetic nanoparticles. As indicated by Zaim and Kerouad [33, 34] are useful models in industrial applications of emerging nanotechnology, which can be used for a variety of nano-devices, due to their reduced size and important magnetic properties such as high density magnetic memories, sensors and molecular imaging devices, etc. Similarly, some of these mixed Ising models as multispin interactions [35] and random crystal field can be used from the experimental point of view, to describe diverse physical systems such as classical fluids, solid ^3H_e, lipid bilayers and rare gases [36]. Furthermore, these mixed Ising models are used to explain experimental results in amorphous ferrimagnetic oxides, wherein F_e^{3+} ions are present [37]. A particularly interesting class of mixed Ising systems are those with relatively high value and half-integer spins, such as spin ($S_i^A = 3/2$, $\sigma_j^B = 5/2$), which have been analyzed less than those of spins of low values [4, 19], and in most cases have been studied with mean field approaches and perturbative methods. These methods, in some cases, have been questioned by discarding all interactions between the spins [38]. Recent studies, based on Monte Carlo methods with finite size scaling analysis, have shown new features of the compportment of the mixed Ising models [5, 39, 40]. In this paper we develop Monte Carlo simulations, reliable technique in solving mixed Ising models [5, 40, 41], to investigate the magnetic properties of a ferrimagnetic system of $S_i^A = 3/2$ and $\sigma_j^B = 5/2$ spins. The model has been studied by various methods, among which highlights the exact recursion rela-

tions [8, 19], mean field theory [4, 42], Monte Carlo [43] and effective field theory [21]. In each of these investigations it is established that the system exhibits a rich variety of multicritical phenomena.

2. Methodology

The model studied is a mixed Ising ferrimagnet with spins $3/2$ and $5/2$, alternating on a square lattice of side $L = 80$. The interaction Hamiltonian of the system is defined as:

$$H = -J_1 \sum_{i,j\epsilon\langle nn\rangle} S_i^A \sigma_j^B - J_2 \sum_{i,k\epsilon\langle nnn\rangle} S_i^A S_k^A - D\sum_{i\epsilon A}(S_i^A)^2 - D\sum_{j\epsilon B}(\sigma_j^B)^2 \quad (1)$$

where S_i^A= $\pm 3/2, \pm 1/2$ and σ_j^B = $\pm 5/2, \pm 3/2, \pm 1/2$, are the spins on the sites of the sublattices A and B, respectively. J_1 is the exchange interaction between pairs of spins to nearest neighbors, J_2 is the exchange parameter between pairs of spins next nearest neighbors of the sublattice A, and D is the crystal field, it causes anisotropy of the system. The first sum is performed over all pairs of spins with nearest neighbor interaction, i.e. between sites with spins $S_i^A = 3/2$ and $\sigma_j^B = 5/2$, the second sum runs over all pairs of spins with next nearest neighbors interaction of spins S_i^A, and sums $\sum_i$ and $\sum_j$ are performed on all sites of spins of the sulattices A and B, respectively. We choose a ferrimagnetic coupling to nearest neighbors, $J_1 < 0$, and we take periodic boundary conditions. All variables in the Hamiltonian are in units of energy.

The simulation of the model is carried out by the Monte Carlo method, generating states ramdomly by a heatbath algorithm, described below. We choose a spin at random, and calculate the energy difference ΔE_{ij} and the transition probability $\exp(-\beta\Delta E_{ij})$ associated with each possible change. Then, is considered whether the spin changes its value, generating a random number θ in the interval $(0, \sum P_i)$, where $\sum P_i$ represents the sum of transition probabilities. The data are generated with 5×10^4 Monte Carlo steps per site after discarding the first 10^4 steps per site to reach equilibrium of the system. Error calculation is estimated using the method of blocks, where the sample L-size is divided in n_b blocks of length $L_b = L/n_b$. When L_b is greater than the correlation length, the averages of the blocks can be considered statistically independent. Thus, the errors are calculated taking the averages of the blocks instead of the original measurements. Error bars are calculated by grouping all the mensurations in 10 blocks and taking the standard deviation [44].

The magnetization per site of the sublattices (M_A, M_B), and the total magnetization per spin, M_T, are defined as:

$$M_A = \frac{2}{L^2}\Big\langle \sum_{i\epsilon A} S_i^A \Big\rangle \quad (2)$$

$$M_B = \frac{2}{L^2}\Big\langle \sum_{j\epsilon B} \sigma_j^B \Big\rangle \quad (3)$$

$$M_T = \frac{M_A + M_B}{2} \quad (4)$$

Defining $\beta = 1/k_B T$, we calculate the specific heat per site, C, by the expression:

$$C = \frac{\beta^2}{L^2}\big(\langle H^2\rangle - \langle H\rangle^2\big) \quad (5)$$

where $\langle H\rangle$ represents the internal energy of the system. An efficient way to locate the compensation temperatures is to find the intersection point of the absolute values of the sublattice magnetizations [45], *i.e.*:

$$|M_A(T_{\text{comp}})| = |M_B(T_{\text{comp}})| \quad (6)$$

with the conditions:

$$sign(M_A(T_{\text{comp}})) = -sign(M_B(T_{\text{comp}})) \quad (7)$$

$$T_{\text{comp}} < T_c \quad (8)$$

3. Results and discussions

In a previous work De la Espriella *et al* [46] obtained several diagrams of ground states of the spin system $(3/2, 5/2)$. Among these, studied the energies and the ground state diagram $J_1 - J_2 - D$ model on the plane $(D/|J_1|, J_2/|J_1|)$. We compare the values of the magnetization, internal energy and specific heat of the system to T = 0K, with those obtained by De la Espriella *et al* [46]. Knowledge of the phase diagrams at $T = 0K$, is important for interpretation the results of the phase diagrams at finite temperature, because are relevants to identify regions where the system could present important magnetic behavior. Then we analyze the effects of crystal field $D^{'} = D/|J_1|$ and the exchange parameter $J_2^{'} = J_2/|J_1|$ on the magnetization, the specific heat per spin, the internal energy, critical and compensation temperatures of the system. To do this, initially we fix the value of $J_2^{'}$ and change the values of $D^{'}$, then $D^{'}$ is fixed and change $J_2^{'}$.

3.1. Crystal Field Effects D

The Fig. 1 indicate the comportment of the total magnetization per spin as functions of temperature, for $D^{'} < 0$ and $J_2^{'} = 3$. Is observed that increasing of the absolute value of the field, entails a diminution of T_{comp}. This behavior in according to reports of Ekiz [47] for a mixed Ising model with spin $S_i^A = 1/2$ and $\sigma_j^B = 1$. Whereas in Fig. 2, growing the crystal field ($D^{'} \geq 0$), implies an increment of the temperatures T_c and T_{comp}. When $D^{'} = 0$, in Fig. 2 is presented the particular model $J_1 - J_2$ and there is a compensation point, implying that the parameter J_2 contributes heavily to the arising of T_{comp}, this behaviour was observed by Buendía *et al* [45] and Dakhama *et al*. [48]. Figures 1 and 2 show that

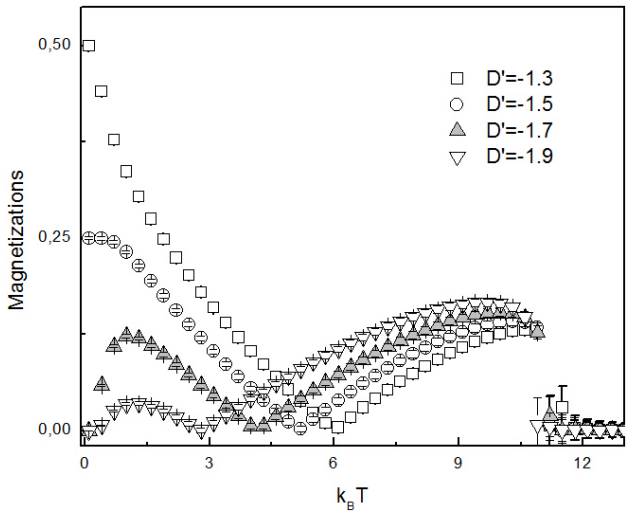

FIGURE 1. Behavior of the magnetization of the system, $|M_T|$, as a function of temperature for $J_2^{'} = 3$ and $D^{'} < 0$.

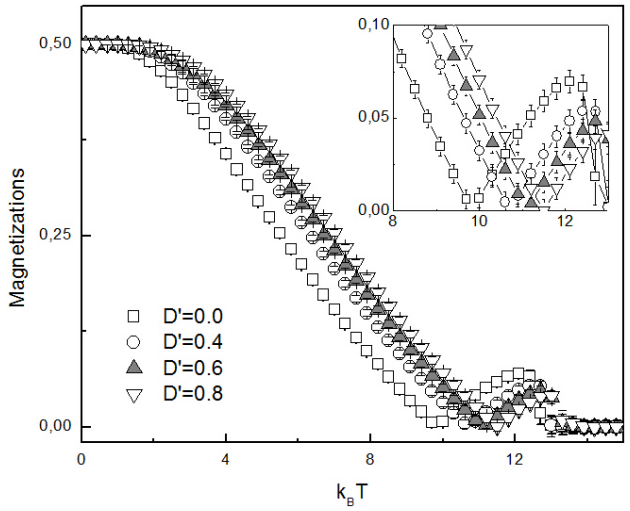

FIGURE 2. Behavior of the magnetization of the system, $|M_T|$, as a function of temperature for $J_2^{'} = 3$ and $D^{'} \geq 0$.

there is a range of values of crystal field in which exist compensation points. When $J_2^{'} = 3$ and $D^{'}$ vary positively or negatively, the system passes through different ground states. When the temperature increases above T_{comp}, the total magnetization first aggrandize until reach a maximum and then decreases until it becomes zero at $T = T_c$. The results of the magnetizations at $T = 0K$, coincide with those reported by De la Espriella *et al* [46] in the phase diagram of ground states (Fig. 4 and Table III of [46]). The upper right inset, in the Fig. 2, shows an enlargement of the region where are located the compensation points.

The compensation phenomenon can be understood by examining Figs. 3 and 4, these display the comportment of $|M_T|$, $|M_A|$ and $|M_B|$, for the particular cases $D^{'} = -1.3$ and $D^{'} = -1.7$. For the range $T < T_{\text{comp}}$, sublattice A is more ordered than the sublattice B due to the ferromagnetic interaction J_2, and the magnetizations of the sublattices have

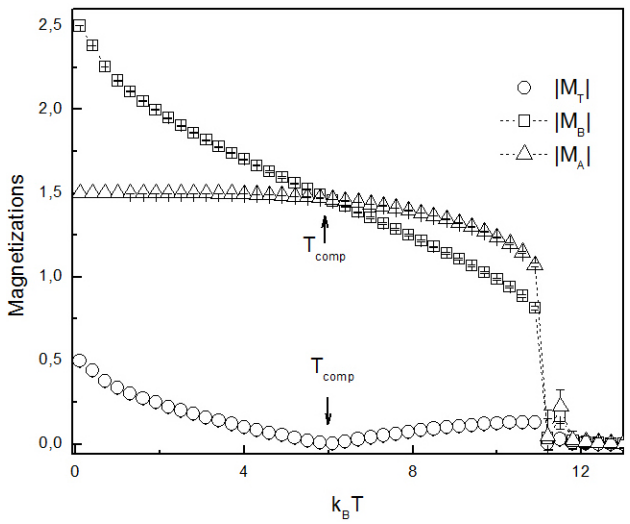

FIGURE 3. Behavior of magnetization per spin of the sublattices $|M_B|$, $|M_A|$ and the total magnetization per spin, $|M_T|$, for $J_2^{'} = 3$ and $D^{'} = -1.3$.

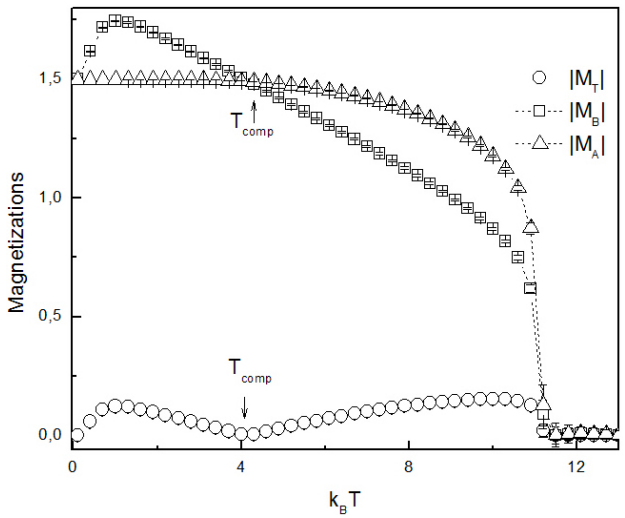

FIGURE 4. Behavior of magnetization per spin of the sublattices $|M_B|$, $|M_A|$ and the total magnetization per spin, $|M_T|$, for $J_2^{'} = 3$ and $D^{'} = -1.7$.

opposite signs, but the cancellation is still incomplete, because there is a residual magnetization in the system produced by J_1, which tends to align the spins close in opposite directions. When the system temperature augment, the residual magnetization direction can change, that is, at this instant prevails the thermal energy, and many spins tend to change the direction, until at $T = T_{\text{comp}}$, sublattices are compensated, *i.e.* $|M_T| = 0$. For $T > T_{\text{comp}}$, both sublattices tend to become disordered, and at $T = T_c$ the system is completely disordered, entering the paramagnetic phase. The compensation effect occurs due to the different rates at which is disordered each of the sublattices, and the antiferromagnetic interaction between them.

We estimate the critical temperatures through the location of the maximum of the specific heats. In Figs. 5 and 6, the

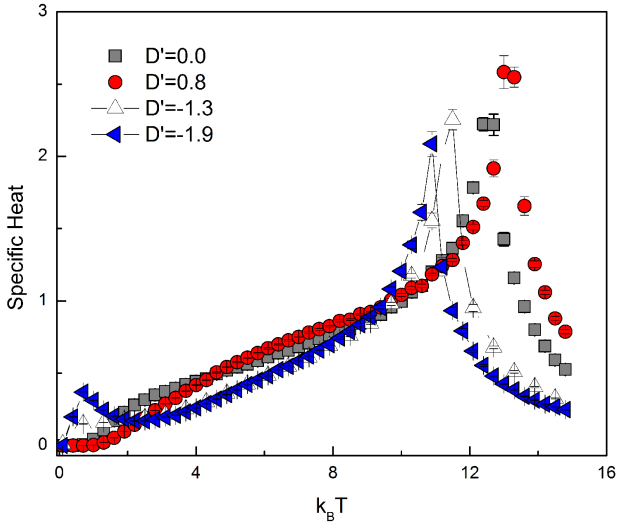

FIGURE 5. Specific heat per spin for different values of $D^{'}$ and $J_2^{'} = 3$.

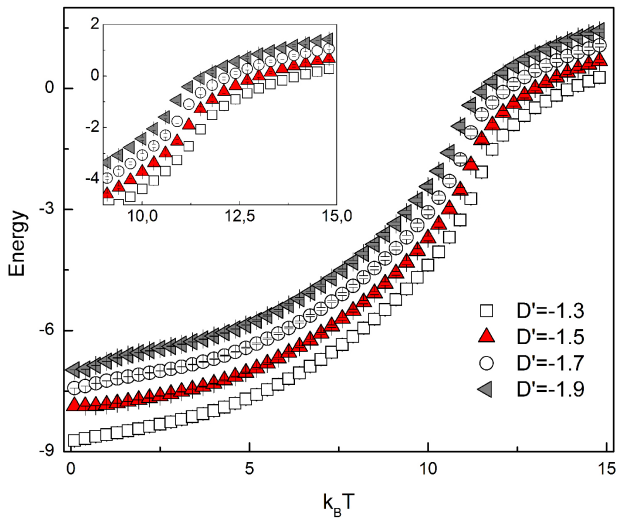

FIGURE 6. Energy per spin for different values of $D^{'}$ and $J_2^{'} = 3$.

the behavior of the specific heat and internal energy per spin are shown, respectively, for varied values of the field $D^{'}$ and $J_2^{'} = 3$. The graphs in the Fig. 5, show that if $|D^{'}|$ ($D^{'} < 0$) raise, the T_c abatement. For $D^{'} = -1.9$, the curve exhibits a second peak at low temperatures, which is considered independent of lattice size and does not correspond to any critical point. This feature was reported by Selke and Oitma [5], exhibiting the effect of the crystal field on the Ising ferrimagnet in a square lattice, in according to our results. The formation of these "anomalous" maximums, occurs when the spins of the sublattice B try to reorganize thermally, because when $T \to 0K$, this sublattice gets disorder very quickly, as shown in Figs. 3 and 4. In the Fig. 6 is obseved that the internal energy per spin increases with the increase of the absolute value of the crystal field $D^{'}$ ($D^{'} < 0$), which is consistent with previous research on mixed Ising systems of spins: 2 and 5/2 [49,50], 1 and 2 [51], and 3/2 and 5/2 [21]. The energy values for $T = 0K$, coincide with those reported in Table III de [46]. For example, when $J_1^{'} = -1$, $D^{'} = -1.7$ and $J_2^{'} = 3$ the system is in region II (Fig. 4 of [46]) with energy $E_0 = -18|J_1| - 9J_2^{'} - 9D^{'} = -7.425$ (Table III of [46]), which is consistent with that exhibited in Fig. 6, for given values of crystal field and exchange parameter $J_2^{'}$. This is a way to check the reliability of our results, hence the importance of ground state diagrams. In the inset in the upper left, you can see how changing the concavity of the curves in the region where the second-order phase transition is present, the temperature at which the magnetizations of the sublattices go to zero continuously, separating the ferrimagnetic phase of the paramagnetic phase. Fig. 7 summarizes the results obtained on the dependence of T_c and T_{comp} with respect to $D^{'}$. In the range of selected values of parameters of the Hamiltonian, critical temperature increases with the crystal field, looking reach a constant value, dependent on the exchange $J_2^{'}$ parameter. For each value of $J_2^{'}$, there is a range of values of $D^{'}$ for which compensation points exist. When $J_2^{'} = 3$, are found compensation temperatures in the range $-2 \leq D^{'} \leq 2$. For the case $J_2^{'} = 5$, compensation points are in the range $-2 \leq D^{'}$. For $D^{'} \approx 21$, T_{comp} is almost independent of crystal field, since it has a constant value that depends heavily on $J_2^{'}$. Notably, while T_c strongly depends of $J_2^{'}$, only the upper limit of T_{comp} depends on $J_2^{'}$.

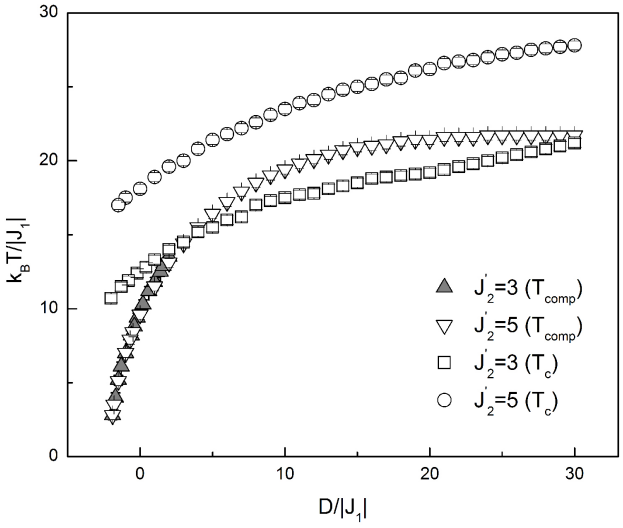

FIGURE 7. Critical (T_c) and compensation (T_{comp}) temperatures, as a function of $D^{'}$.

3.2. Interaction Effects $J_2^{'}$

To analyze the effect of $J_2^{'}$, is fixed $D^{'} = -1.9$ and vary $J_2^{'}$. The Fig. 8 evidence the total magnetization per spin as a function of temperature for different values of $J_2^{'}$, and Fig. 9 testify to the behavior of the total magnetization and the sublattices, as a function of temperature for the specific case $J_2^{'} = 2$. In Fig. 8 we see that once appears T_{comp}, this depends very weakly of $J_2^{'}$, otherwise to the T_c, which mark-

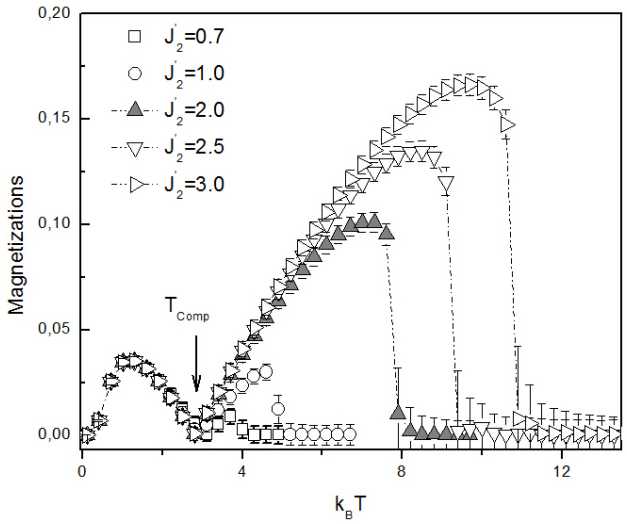

FIGURE 8. Total magnetizations per spin as a function of temperature for $D^{'} = -1.9$ and $J_2^{'} > 0$.

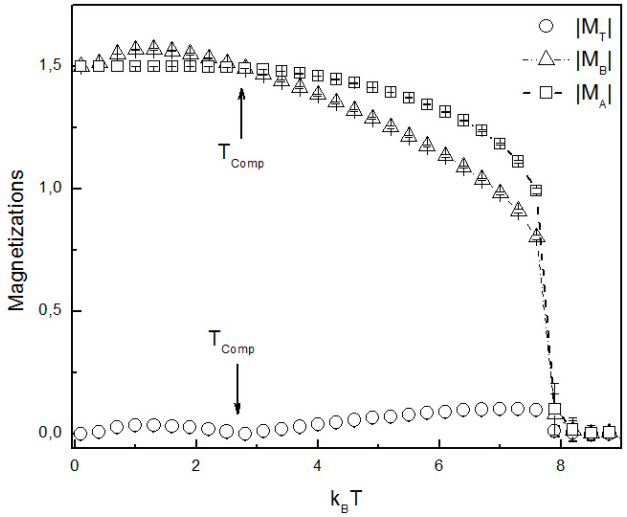

FIGURE 9. Behavior of magnetization per spin of the sublattices $|M_B|, |M_A|$ and the total magnetization per spin, $|M_T|$, for $J_2^{'} = 2$ and $D^{'} = -1.9$.

edly augment with the increase of the parameter $J_2^{'}$ exchange. A special feature, shown in Fig. 8, is that the deportment of the total magnetization for $T < T_{\text{comp}}$ is independent of the value of $J_2^{'}$, whereas for $T > T_{\text{comp}}$ maximum value of the total magnetization rise with $J_2^{'}$ increased.

With reference to Fig. 9 is observed that $|M_A|$ falls from its saturation value (1.5) at $T = 0K$, until it becomes zero at $T = T_c$, indicating that the sublattice A remains ferromagnetic more ordered than the sublattice B, by $J_2^{'}$ interaction effects, whereas $|M_B|$ decays more rapidly. The $|M_A|$ plot has a similar comportment to the recently reported by Selke and Ekiz [40], about the study of Ising ferrimagnets in square lattice with next nearest neighbors coupling. Again the existence of T_{comp} is due to the different decay rates of magnetizations of the sublattices. Specific heat curves, shown in Fig. 10, indicate that the critical temperature, estimated at the

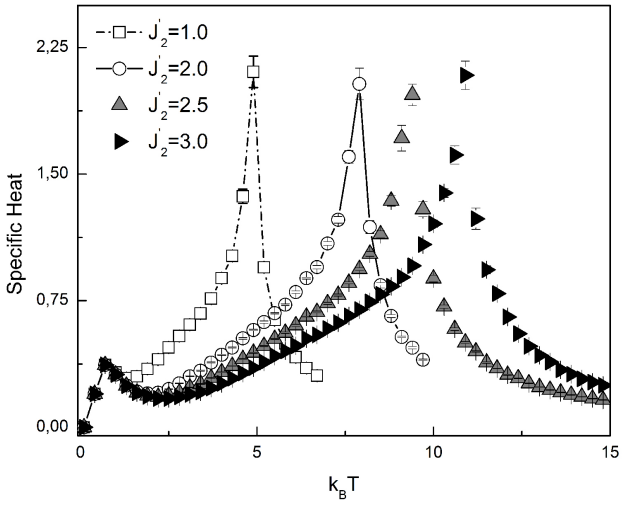

FIGURE 10. Specific heat per spin for different values of $J_2^{'}$ and $D^{'} = -1.9$.

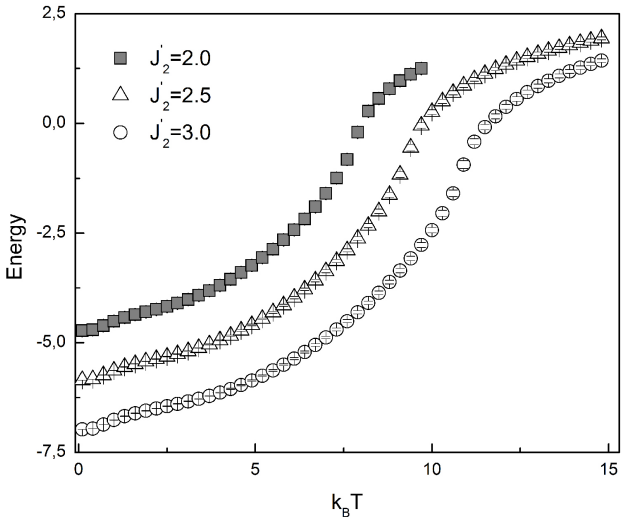

FIGURE 11. Energy per spin for $J_2^{'} > 0$ and $D^{'} = -1.9$.

the maximum of the curves, aggrandize with increasing $J_2^{'}$ and the peaks shift to the high temperature region.

We can see at low temperatures, a thermal rearrangement of the spins of the sublattice B for the crystal field effect. Figure 11 exhibit the deportment of the energy per spin of the system. There is a change of concavity of the curves in the critical region. Minimum energy for each value of $J_2^{'}$, in according with the ground state of the model depicted in Fig. 4 in [46]. As you increase the value of the interaction $J_2^{'}$, the internal energy of the system decreases, this is consistent with previous investigations [21, 49–51]. Critical behavior of the system as a function of $J_2^{'}$, is summarized in Fig. 12. Above a minimum value $J_2^{'}$, which depends on the crystal field, the compensation temperature is almost independent of the value of $J_2^{'}$ and has a constant value which depends strongly on $D^{'}$. In contrast, we find that the critical temperature augment linearly with $J_2^{'}$, and is practically independent of the crystal

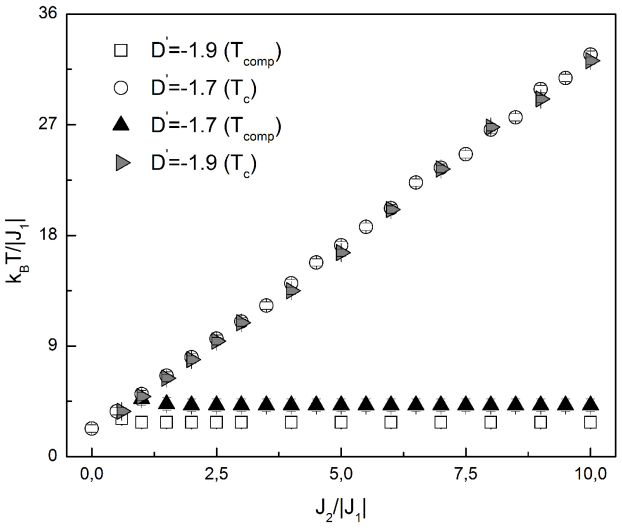

FIGURE 12. Critical (T_c) and compensation (T_{comp}) temperatures, as a function of $J_2^{'}$.

field value. For $D^{'} = -1.9$, the range of values of parameter $J_2^{'}$ where exist T_{comp} is $J_2^{'} \geq 0.6$ and for $D^{'} = -1.7$ is $J_2^{'} \geq 1$. This tells us that minimum value of $J_2^{'}$ for which exists T_{comp} decreases, by increasing the absolute value of $D^{'}$.

4. Conclusion

We develop a numerical study of the magnetic comportment of a ferrimagnetic mixed Ising model of spins $S_i^A = 3/2$ and $\sigma_j^B = 5/2$, alternating on a square lattice. When the Hamiltonian includes antiferromagnetic interactions to nearest neighbors, ferromagnetics to next nearest neighbors on sublattice A, and crystal field, exists a range of parameter values where the system presents T_{comp}. We calculated the phase diagrams at finite temperature of the internal energy, $|M_T|$, $|M_A|$, $|M_B|$ and the specific heat, indicating the T_{comp} and T_c for various combinations of parameters. To $J_2^{'}$ fixed, T_c augment with $D^{'}$ to reach a limit value that depends on the field. The T_{comp} increases rapidly with $D^{'}$, but its value is independent of $J_2^{'}$, since it has a constant value which depends markedly on this parameter ($J_2^{'} = 5$). When $D^{'}$ is fixed, the T_c raise linearly with $J_2^{'}$, but is almost independent of $D^{'}$, whereas T_{comp} occurs when $J_2 > J_{2\text{min}}(D)$ and its value depends only on D. We found T_{comp} in the particular case $J_1 - J_2$, indicating that the parameter J_2 strongly influences the occurrence of compensation points. Finally, is evident that increasing $J_2^{'}$ increases the range of T_{comp} and increases T_c.

1. M. Keskin, O. Canko and S. Güldal, *Phys. Lett. A* **374** (2009) 1.
2. M. Keskin and E. Kantar, *J. Magn. Magn. Mater.* **322** (2010) 2789.
3. B. Deviren, M. Keskin and O. Canko, *J. Magn. Magn. Mater.* **321** (2009) 458.
4. B. Deviren and M. Keskin, *J. Stat. Phys.* **140** (2010) 934.
5. W. Selke and J. Oitmaa, *J. Phys.: Condens. Matter* **22** (2010) 076004.
6. J. N. Behera, D. M. D'Alexandro, M. Soheilnia and J. R. Long, *Chem. Mater.* **21** (2009) 1922.
7. C. Ekiz, *Physica A* **387** (2008) 1185.
8. R. A. Yessoufou, S. H. Amoussa and F. Hontinfinde, *Cent. Eur. J. Phys.* **7** (2009) 555.
9. Y. Nakamura and J. W. Tucker, *IEEE Transactions on Magnetics* **38** (2002) 2406.
10. M. Keskin and Y. Polat, *J. Magn. Magn. Mater.* **321** (2009) 3905.
11. S. Ohkoshi and K. Hashimoto, *Electrochem. Soc. Interface* **11** (2002) 34.
12. E. Albayrak and S. Yilmaz, *Physica A* **387** (2008) 1173.
13. S. J. Blundell and F. L. Pratt, *J. Phys.: Condens. Matter* **16** (2004) 771.
14. D. Gatteshi and R. Sessoli, *J. Magn. Magn. Mater.* **272** (2004) 1030.
15. D. Subhabrata, O. Brandt, M. Ramsteiner, V. F. Sapega and K. H. Ploog, *Phys. Rev. Lett.* **94** (2005) 037205.
16. J. S. Miller and M. Drillon. *Magnetism: Molecules to Materials V* (Wiley-VCH, New York, 2004).
17. J. Strecka, *Physica A* **360** (2006) 379.
18. C. Ekiz, *Physica A* **347** (2005) 353.
19. E. Albayrak and A. Yigit, *Phys. status solidi b* **244** (2007) 748.
20. T. Kaneyoshi, *Physica A* **286** (2000) 518.
21. Q. Zhang, G. Wei and Y. Gu, *Phys. status solidi b* **242** (2005) 924.
22. A. Zaim, M. Kerouad and Y. Belmamoun, *Physica B* **404** (2009) 2280.
23. G. M. Buendía and J. Villarroel, *J. Magn. Magn. Mater.* **310** (2007) E495.
24. G. Chern, L. Horng, W. K. Shieih and T. C. Wu, *Phys. Rev. B* **63** (2001) 094421.
25. H. Kageyama, D. I. Khomskii, R. Z. Levitin and A. N. Vasil'ev, *Phys. Rev. B* **67** (2003) 224422.
26. L. Néel, *Ann. Phys.* **3** (1948) 137.
27. M. Multigner, S. Lakamp, G. Pounoy, A. Hernando and R. Valenzuela, *Appl. Phys. Lett.* **696** (1996) 2761.
28. G. M. Buendía and E. Machado, *Phys. Rev. B* **61** (2000) 14686.
29. S. Ohkoshi, A. Yukinori, F. Akira and K. Hashimoto, *Phys. Rev. Lett.* **82** (1999) 1285.
30. M. Mansuripur, *J. Appl. Phys.* **61** (1987) 1580.
31. S. A. Chavan, R. Granguly, V. K. Jain and J. V. Yakhmi, *J. Appl. Phys.* **79** (1996) 5260.

32. C. Mathoniere, C. J. Nuttall, S. G. Carling and P. Day, *Inorg. Chem.* **35** (1996) 1201.
33. A. Zaim, M. Kerouad, *Physica A* **389** (2010) 3435.
34. C. J. O'Connor, J. Tang and H. Zhang, in: J.S. Miller, M. Drillon (Eds) *Magnetism: Molecules to Materials III*. (Wiley-VCH, Weinheim, 2002) p.1.
35. A. Zaim, M. Kerouad and Y. Belmamoun, *Physica B* **404** (2009) 2280.
36. N. Benayad and M. Ghliyem, *Physica B:* **407** (2012) 6.
37. K. Htoutou, A. Ainane and M. Saber. *J. Magn. Magn. Mater.* **269** (2004) 245.
38. B. Deviren, M. Keskin and O. Canko, *Physica A* **388** (2009) 1835.
39. M. Zukovic and A. Bobak, *Physica A* **389** (2010) 5402.
40. W. Selke and C. Ekiz, *J. Phys.: Condens. Matter* **23** (2011) 496002.
41. M. Godoy, V. Souza and W. Figueiredo, *Phys. Rev. B* **69** (2004) 054428.
42. H. Mohamad, *J. Magn. Magn. Mater.* **323** (2011) 61.
43. S. J. Luo, Z. D. He and Q. L. Jie, *J. Magn. Magn. Mater.* **321** (2009) 3396.
44. M. E. Newman and G. T. Barkema, *Monte Carlo Methods in Statistical Physics.* (Oxford University Press, New York, 2006).
45. G. M. Buendía and M. A. Novotny, *J. Phys.: Condens. Matter* **168** (1997) 105.
46. N. De La Espriella and G. M. Buendía, *Physica A* **389** (2010) 2725.
47. C. Ekiz, *J. Magn. Magn. Mater* **293** (2005) 759.
48. A. Dakhama and N. Benayad, *J. Magn. Magn. Mater.* **213** (2000) 117.
49. Y. Nakamura, Phys. Rev. B **62** (2000) 11742.
50. Q. Zhang and G. Z. Wei, *J. Magn. Magn. Mater.* **253** (2002) 96.
51. Q. Zhang, G. Z. Wei and Z. Xin, Y. Liang, *J. Magn. Magn. Mater.* **280** (2004) 14.